



THE UNIVERSITY *of* EDINBURGH

Edinburgh Research Explorer

## Aged Mice Demonstrate Greater Muscle Degeneration of Chronically Injured Rotator Cuff

**Citation for published version:**

Sharma, AK, Levian, B, Shah, P, Mosich, GM, Husman, R, Ariniello, A, Gatto, JD, Hu, VJ, McClintick, DJ, Jensen, AR, McAllister, DR, Péault, B, Dar, A & Petrigliano, FA 2019, 'Aged Mice Demonstrate Greater Muscle Degeneration of Chronically Injured Rotator Cuff', *Journal of Orthopaedic Research*.  
<https://doi.org/10.1002/jor.24468>

**Digital Object Identifier (DOI):**

[10.1002/jor.24468](https://doi.org/10.1002/jor.24468)

**Link:**

[Link to publication record in Edinburgh Research Explorer](#)

**Document Version:**

Peer reviewed version

**Published In:**

Journal of Orthopaedic Research

**Publisher Rights Statement:**

This is the author's final peer-reviewed manuscript as accepted for publication.

**General rights**

Copyright for the publications made accessible via the Edinburgh Research Explorer is retained by the author(s) and / or other copyright owners and it is a condition of accessing these publications that users recognise and abide by the legal requirements associated with these rights.

**Take down policy**

The University of Edinburgh has made every reasonable effort to ensure that Edinburgh Research Explorer content complies with UK legislation. If you believe that the public display of this file breaches copyright please contact [openaccess@ed.ac.uk](mailto:openaccess@ed.ac.uk) providing details, and we will remove access to the work immediately and investigate your claim.



1 **Aged Mice Demonstrate Greater Muscle Degeneration of Chronically Injured Rotator Cuff**

2 Abhinav K. Sharma<sup>1</sup>, Brandon Levian<sup>1</sup>, Paras Shah<sup>1</sup>, Gina M. Mosich<sup>1</sup>, Regina Husman<sup>1</sup>, Allison  
3 Ariniello<sup>1</sup>, Jonathan D. Gatto<sup>1</sup>, Vivian J. Hu<sup>1</sup>, Daniel J. McClintick<sup>1</sup>, Andrew R. Jensen<sup>1</sup>, David  
4 R. McAllister<sup>1</sup>, Bruno Péault<sup>1,2</sup>, Ayelet Dar<sup>1,\*</sup> and Frank A. Petrigliano<sup>1,\*</sup>

5

6 <sup>1</sup>David Geffen School of Medicine, Orthopaedic Hospital Research Center. University of California, Los  
7 Angeles, CA, USA

8 <sup>2</sup>Center for Cardiovascular Science and MRC Centre for Regenerative Medicine, University of Edinburgh,  
9 UK

10 \*Co-senior authors

11

12 Corresponding author: Address correspondence to Frank A. Petrigliano, MD, UCLA Department  
13 of Orthopaedic Surgery, CHS 76-143, Los Angeles, CA, 90095. Phone: 310-825-2126. Fax: 310-  
14 825-1311 Email: FPetrigliano@mednet.ucla.edu

15 Running title: Age-Related Degeneration of Rotator Cuff

16

17 Author Contribution Statement: A.K.S performed RT-PCR, *in vitro* studies and imaging, analyzed  
18 data, and wrote sections of the manuscript. B.L performed RT-PCR and data analysis. P.S assisted  
19 with *in vitro* experiments, and imaging. G.M. performed mouse surgeries. R.H., J.D.G., V.J.H.,  
20 and D.J.M assisted with data analysis. A.A. performed RT-PCR. A.R.J. and D.R.M. reviewed and  
21 wrote sections of the manuscript. B.P., A.D., and F.A.P. monitored project design, manuscript  
22 review, revision and approval. All authors have read and approved the final submitted manuscript.

23 **ABSTRACT**

24 Massive tears of the rotator cuff are often associated with progressive and irreversible muscle  
25 degeneration due to fibrosis, fatty infiltration, and muscle atrophy. Rotator cuff tears are common  
26 in individuals older than 60 years and the repair of these tears ~~are~~ is amongst the most prevalent  
27 of orthopaedic procedures. However, most current models of this injury are established in  
28 ~~physiologically~~ young animals, which may not accurately recapitulate the clinical condition. In  
29 this study we used a murine model of massive rotator cuff tears to evaluate age-related muscle  
30 degeneration following chronic injury. The expression of the fibro-adipogenic genes encoding  
31 collagen type III and leptin was higher in aged rotator cuff compared to matched injured young  
32 tissue at 2 weeks post-injury and development of fibrosis was accelerated in aged mice within 5  
33 days post-injury. Furthermore, synthesis of collagens type I and -III and fat tissue accumulation  
34 were significantly higher in injured rotator cuffs of aged mice. Similar frequency of fibro-  
35 adipogenic PDGFR $\beta$ <sup>+</sup>PDGFR $\alpha$ <sup>+</sup> progenitor cells was measured in non-injured rotator cuff of aged  
36 and young mice, but PDGFR $\beta$ <sup>+</sup>PDGFR $\alpha$ <sup>+</sup> cells contributed to significantly larger fibrotic lesions  
37 in aged rotator cuffs within 2 weeks post-injury, implying a more prevalent fibrotic environment  
38 in the aged injured muscle. Altogether, these findings demonstrate age-dependent differences in  
39 rotator cuff response to chronic injury with a more profound fibro-adipogenic change in aged  
40 muscles. Clinically, cell therapies for muscular pathologies should not only consider the cell type  
41 being transplanted but also the recipient milieu into which these cells are seeded.

42

43 **Keywords:** rotator cuff tear; aging; skeletal muscle; fibrosis; fatty degeneration; fibro-adipogenic  
44 progenitor cell

45

46 **INTRODUCTION**

47 Rotator cuff (RC) tears are increasingly common in individuals older than 60 years and  
48 treatment and repair of tears are amongst the most prevalent of orthopaedic procedures.<sup>1</sup> Even with  
49 advancements in techniques and procedures for repair, re-tear rates have been shown to range from  
50 11 to 57% depending on factors such as patient age, large tear size and tendon degeneration,<sup>2-5</sup> and  
51 muscle atrophy and fatty infiltration in the RC muscles leading to reduced healing potential of the  
52 RC.<sup>6</sup> More than half of the population older than 70 years will develop full-thickness RC tears,  
53 which can impact quality of life and adversely affects daily functioning.<sup>6,7</sup> Elderly patients also  
54 tend to have diminished healing potential and effectiveness of RC repair due to the aforementioned  
55 factors, as well as generally having more comorbidities and a -propensity for larger RC tears and  
56 more substantial tendon degeneration.<sup>6,8-11</sup> Thus, outcomes of -RC repair surgeries are poorer in  
57 this population due in large part to increased re-tear rates and RC healing failure and subsequent  
58 loss of strength and decreased function.<sup>6,8-10</sup>

59 A positive correlation exists between age and RC tissue degeneration, prevalence of full  
60 thickness tears, and tear size, indicated by the number of tendons involved.<sup>12,13</sup> These data suggest  
61 that the increased prevalence of RC pathology with age is a function of persistent RC degeneration  
62 over time. Despite the significance of this issue, the age-related pathophysiological mechanisms  
63 underlying the degenerative changes in older RC tissue have yet to be elucidated.<sup>14</sup>

64 Regenerative therapies using stem and progenitor cells may be employed to enhance  
65 healing and diminish the effect of fatty infiltration and muscle atrophy following RC tears.<sup>15</sup>  
66 Myogenic progenitor cells may not only reduce muscle atrophy but may also foster regeneration  
67 of muscle tissue.<sup>16</sup> Murine models have been established for studying the effects of chronic RC  
68 tears and subsequent fatty degeneration to gain a better understanding of the pathophysiologic

69 changes that occur in aging human RC muscles.<sup>17</sup> Additionally, small animal models are being  
70 used to study stem cell injection as well as the tissue and gene expression profiles of RC tears in  
71 humans.<sup>15, 16</sup> Mice can incur pathological changes post supraspinatus and infraspinatus tissue  
72 transection and denervation of the suprascapular nerve (TTDN) similar to those seen in humans  
73 following massive RC tears.<sup>18</sup> In this study we compared RC remodeling and degeneration,  
74 histologically and with respect to gene expression, between young and old mice following TTDN  
75 to determine the validity of using either age group as models for massive RC injury. In mice,  
76 senescence starts around 18 months, when the biomarkers of old age are detected.<sup>19</sup> Accordingly,  
77 we used ~~old~~ mice ranging from 18 to 24 months of age, which matches humans ranging from 56  
78 to 75 years. We found increased fibrosis and fat accumulation in old non-injured and chronically  
79 injured RC muscles in comparison to young RC muscle. Additionally, the frequency of interstitial  
80 PDGFR $\beta$ <sup>+</sup>PDGFR $\alpha$ <sup>+</sup> fibro-adipogenic progenitor cells was similar between non-injured young and  
81 old muscle. However, a substantial increase in PDGFR $\beta$ <sup>+</sup>PDGFR $\alpha$ <sup>+</sup> cells populating fibrotic  
82 lesions was measured in old RC within 6 weeks post TTDN.

**Commented [PB1]:** These are largely perivascular; not only interstitial

83  
84  
85  
86  
87  
88  
89  
90  
91  
92

93 **METHODS**

94 **Mice**

95 PDGFR $\beta$ -Cre mice were crossed with mTmG (tdTomato-EGFP) mice. C57/BL6J mice were used  
96 as PDGFR $\beta$ -Cre mice matched wild type strain. All animal procedures were approved by the local  
97 Institutional Animal Care and Use Committee (IACUC). Mice at the age of 3-4 months were  
98 considered young and mice older than 18 months were considered old.<sup>19, 20</sup>

99

100 **Rotator Cuff Injury Model**

101 We induced massive RC tears in old and young mice. We anesthetized the mice with 2% isoflurane  
102 and oxygen, administered buprenorphine for analgesia, and sterilely prepared and draped the right  
103 shoulder. A 1-cm longitudinal skin incision was made over the right glenohumeral joint to access  
104 the deltoid fibers, which were then split directly posterior to the deltoid tuberosity longitudinally  
105 to reach the supraspinatus and infraspinatus tendons. These tendons were isolated and sharply  
106 detached from their insertions on the greater tuberosity; additionally, the distal 5 mm of each  
107 tendon was resected to prevent scar formation to the humerus. Next, the suprascapular nerve was  
108 identified through a 5 mm incision in the trapezius musculature anterior to the lateral scapula and  
109 cut for the denervation procedure. Lastly, a 5-0 Vicryl (Ethicon, Somerville, NJ, USA) suture was  
110 used to close the deltoid muscle and skin.

111

112 **Histology and Immunohistochemistry**

113 Infraspinatus and supraspinatus muscles were fixed in 4% formalin, embedded in paraffin,  
114 sectioned, dehydrated, and stained with hematoxylin and eosin for general tissue structure analysis  
115 or picrosirius red for collagen expression according to manufacturer instructions (Abcam,  
116 Cambridge, UK). Both muscles, supraspinatus and infraspinatus were always prepared for

117 histology in the same orientation and sectioned in the axial plane and all multiple sections from a  
118 single muscle were 5  $\mu$ m thick. Images were acquired with an Axio Imager 2 light microscope  
119 (Zeiss, Oberkochen, Germany). For histological examination, injured young and old cohorts were  
120 divided into 3 groups and analyzed at 5 days, 2 weeks and 6 weeks post operation (n = 3 mice per  
121 group). Non-injured young and old mice were used as controls (n = at least 3 mice per group). For  
122 fluorescence microscopy, frozen sections were fixed with 4% paraformaldehyde, washed 3 times  
123 in PBS, immunolabeled with rabbit anti-mouse PDGFR $\beta$  and goat anti-mouse PDGFR $\alpha$  overnight  
124 at 4°C, washed 3 more times in PBS, and then incubated with Alexa Fluor 647-conjugated, donkey  
125 anti-rabbit and Alexa Fluor 405-conjugated, donkey anti-goat secondary antibodies (Abcam).  
126 DAPI (4'6-diamino-2-phenylindole dihydrochloride, 1:1000, Molecular Probes, Waltham, MA)  
127 was used for nuclei labeling. Images and movies were acquired with the Axio Imager 2 light  
128 microscope. For immunohistochemical analysis, injured young and old cohorts were divided into  
129 3 groups and analyzed at 5 days, 2 weeks and 6 weeks post operation (n = 3 mice per group). Non-  
130 injured young and old mice were used as control (n = 3 mice per group).

131

### 132 **Quantification of Fibrosis and Adipocytes**

133 Following picrosirius red staining as described above, fibrosis was quantified in injured and non-  
134 injured, young and old tissue sections by red pixel intensity measurement by Photoshop and the  
135 fraction of fibrosis was calculated by dividing the number of red pixels by the entire number of  
136 pixels per area. Adipocytes were counted in hematoxylin and eosin stained RC sections for  
137 quantification of fat content. Based on our observations that RC degeneration spreads laterally,  
138 images were not taken randomly; instead, the whole area of each section was screened and all  
139 fibrotic or adipogenic regions were imaged at the same magnification of x200. Therefore, the

140 number of images per section varied based on the relative size of the fibrotic or the adipogenic  
141 area.

142

### 143 **RNA Extraction and Reverse Transcription PCR**

144 The infraspinatus and supraspinatus muscle tissues were immediately frozen and stored at -80°C  
145 following harvest. RNA was isolated from muscle tissue using ADD KIT and its concentrations  
146 were measured with NanoDrop (Thermo Fisher Scientific, Waltham, MA). The RNA was then  
147 reverse transcribed to complementary DNA using the iScript cDNA Synthesis Kit (BioRad,  
148 Hercules, CA) and the iCycler thermal cycler (BioRad). We ran the PCRs using 130-200 ng of  
149 RNA under the following cycling conditions: 5 min at 25°C for priming, followed by 20 min at  
150 46°C for reverse transcription, and finally, 1 min at 95°C for reverse transcriptase inactivation. We  
151 quantified the complementary DNA using Absolute SYBR Green Low ROX qPCR Mix (Life  
152 Technologies, Carlsbad, CA) and the ViiA 7 Real-Time PCR System (Applied Biosystems, Foster  
153 City, CA) using the following cycling conditions: 15 min at 95°C for enzyme activation, followed  
154 by 40 cycles of amplification (15 s at 95°C, 30 se at 60°C, and 30 s at 72°C). Gene expression  
155 profiles were determined by analyzing quantitative RT-PCR data of collagen and leptin genes by  
156 calculating the fold change ( $2^{-\Delta\Delta Ct}$ ) in gene expression compared to the expression of the  
157 housekeeping gene GAPDH. Primer sequences (Integrated DNA Technologies, Coralville, IA)  
158 used for RT-PCR: GAPDH-F CCTGGAGAAACCTGCCAAGTATG, GAPDH-R  
159 AGAGTGGGAGTTGCTGTTGAAGTC; leptin-F TCCTGTGGCTTTGGTCCTATC, leptin-R  
160 ATACCGACTGCGTGTGTGAA; Col3A1-F AGGCTGAAGGAAACAGCAAAA, Col3A1-R  
161 TAGTCTCATTGCCTTGCGTG. For RT-PCR analysis, cohorts were divided into 3 groups and  
162 analyzed at 5 days, 2 weeks and 6 weeks post operation. Non-injured young and old mice were  
163 used as controls.



164 **Flow Cytometry**

165 Non-injured young (n=3, 3-4 months) and old (n=3, 18-20 months) RC muscles were excised,  
166 mechanically minced, and dissociated using 0.5 mg/mL collagenase II and dispase (Sigma, St  
167 Louis, MO, USA) in Dulbecco's modified Eagle's medium (DMEM) supplemented with 10% fetal  
168 bovine serum (FBS) and 1% penicillin-streptomycin (Pen-Strep) for 30 min at 37°C on a shaker.  
169 Freshly isolated cells were washed in PBS, centrifuged, and labeled with PE/Cy7-conjugated anti-  
170 mouse PDGFR $\alpha$  and APC-conjugated anti-mouse PDGFR $\beta$  (eBioscience, San Diego, CA)  
171 according to the manufacturer's instructions. We used the LSR II and FACSDiva flow cytometers  
172 (BD Biosciences, San Jose, CA) for subsequent analyses.

173

174 **Statistical Analysis**

175 All data are presented as mean+SEM. Single factor ANOVA was used to compare mean values  
176 among study groups (Excel 2010) [and two-way ANOVA was used to analyze effects of injury and](#)  
177 [age on gene expression](#). We controlled the family-wise error rate by using a Bonferroni correction.  
178 For all analyses, a *P* value of  $\leq 0.01$  was considered statistically significant.

179

180

181

182

183

184

185

186

187 **RESULTS**

188 **Irreversible Nerve and Tendon Transection Induces Degeneration of Young and Old Murine**  
189 **RC**

190 To evaluate the changes in muscle tissue morphology following induction of chronic  
191 muscle injury by nerve and tendon transection (TTDN), RC muscle was harvested from young (2-  
192 4 months) and old mice (20-24 months) at early (5 days), intermediate (2 weeks) and late (6 weeks)  
193 stages of muscle remodeling post-injury. Histological examination of hematoxylin and eosin  
194 stained sections of non-injured and injured RC from young and old mice revealed that, in  
195 comparison to the normal appearance of healthy young (Fig. 1A) and old muscle (Fig. 1E), TTDN  
196 induced a robust increase in muscle cellularity accompanied by myofiber necrosis within 5 days  
197 regardless of mouse age (Fig. 1B and F). At 2 weeks post-TTDN, myocyte regeneration was  
198 observed with an increase in myofibers with central nuclei, a hallmark of the regenerative process.  
199 Additionally, the accumulation of fat cells was seen in both young (Fig. 1C) and old (Fig. 1G) RC,  
200 and this fatty infiltration was greater at this time point relative to the 5-day tissue samples. Six  
201 weeks after TTDN, histology of both the young (Fig. 1D) and old (Fig. 1H) RC tissues revealed  
202 fibro-adipogenic changes, which were more pronounced in the old RC tissue.

203

204 **Development of Fibrosis is Accelerated in Chronically Injured RC of Old Mice**

205 Development of fibrosis is defined by increased deposition of collagens type I and III and  
206 was evaluated by quantification of red pixel intensity after picrosirius red staining of RC muscle  
207 sections. Progressive increase in collagen content was measured in both old and young injured RC  
208 within 6 weeks post-TTDN (Fig. 2I). Quantification of picrosirius red staining revealed that  
209 collagen content was higher in non-injured old RC (n=3, 20-21 months) compared to non-injured

210 young RC (n=4, 3-4 months,  $p<0.005$ ), and that collagen accumulation in fibrotic lesions was  
211 significantly greater in old injured RC at 5 days (n=3, 22 months,  $p<0.001$ ) and 2 weeks (n=3, 20-  
212 22 months,  $p<0.005$ ) post-TTDN in comparison to young RC (Fig. 2I), indicating accelerated  
213 fibrogenesis in chronically injured old RC muscle. The 6-week post-TTDN young (n=3, 3-4  
214 months) and old (n=3, 20-22 months) tissues had the most pronounced fibrotic change overall  
215 compared to earlier time points after injury of each age group (Fig. 2I,  $p<0.01$ ), the old RC tissue  
216 demonstrating more collagenous infiltration than the young RC. [There was no significant](#)  
217 [interaction between mouse age and injury on collagen synthesis \(two-way ANOVA,  \$p<0.01\$ \).](#)

218 Quantitative PCR of collagen III expression coincided with the observed increase in  
219 fibrosis that was quantified for non-injured old RC muscle ( $p<0.005$ ) as well as over time for both  
220 the young and old RC tissues following TTDN (Fig. 2J). **In both old and young RC,** expression of  
221 collagen III was induced by injury within 5 days (n=5, 20-22 months,  $p<0.01$ ), escalated at 2 weeks  
222 post-injury (n=3, 20-22 months) and significantly declined at 6 weeks post-TTDN (n=5, 20-25  
223 months,  $p<0.005$ ), when both the young and old tissues had already become progressively more  
224 fibrotic. Synthesis of collagen I peaked at 5 days post injury in young injured RC and lasted longer  
225 in old RC peaking at 2 weeks after injury in old RC (Fig. 2K). The relative expression pattern of  
226 matrix metalloproteinase 2 (MMP2) was similar to that of collagen I (Fig. 2L) with the expression  
227 of both genes declining at 6 weeks post-TTDN (Fig. 2K-L). [A two-way ANOVA revealed](#)  
228 [significant interaction between mouse age and injury on gene expression levels of collagen I](#)  
229 [\( \$F\_{3,26}=7.6\$ ,  \$p<0.01\$ \) and MMP-2 \( \$F\_{3,24}=6.99\$ ,  \$p<0.01\$ \).](#)

**Commented [PB2]:** But all results described in the sentence are in old mice

### 233 **Greater Fat Tissue Accumulation is Observed in Chronically-Injured Old RC**

234 To assess age-related differences in muscle tissue fatty degeneration following massive RC  
235 tear, we performed TTDN on old and young mice and analyzed post-injury adipogenesis at various  
236 time points. Histological analysis revealed that while adipocytes were rarely detected in non-  
237 injured young (n=4, 3-4 months, Fig. 3A) and old (n=3, 20-21 months, Fig. 3E) RCs, small  
238 adipocyte clusters were seen in injured young and old RC within 5 days (n=5, Figs. 3B and 3F)  
239 and 2 weeks (n=3) post-TTDN. Robust increase in fat tissue accumulation was observed in both  
240 young and old RC tissues at 2 weeks (Figs. 3C and 3G,  $p<0.001$ ) and 6 weeks following TTDN  
241 (Fig. 3D and 3H,  $p<0.001$ ). No significant increase was found in adipocyte numbers between  
242 injured young and old RC at 5 days post-TTDN (Fig. 3I). However, considerably more adipocytes  
243 were counted in old injured RC (n=3, 3-4 months) in comparison to young RC at 2 and 6 weeks  
244 (n=4, 20-22 months) post-TTDN (Fig. 3I,  $p<0.01$ ), implying that the degenerated  
245 microenvironment of old RC promotes accelerated growth of adipose tissue at late stages of  
246 chronic injury. [Two-way ANOVA revealed significant interaction between mouse age and injury  
247 on adipocyte count \( \$F\_{3,152}=6.28\$ ,  \$p<0.01\$ \).](#)

248 Gene expression of leptin (Fig. 3J), a hormone that is released from fat cells, was  
249 progressively elevated in both young and old degenerating RC (Fig. 3J) and coincided with the  
250 increase in the numbers of adipocytes that were quantified over time for both the young and old  
251 RC tissues following TTDN (Fig. 3I). At 6 weeks post-TTDN, old RC demonstrated the highest  
252 levels of leptin gene expression (Fig. 3J), corresponding with higher adipocyte number in old RC  
253 in comparison to young RC at the same time point post-TTDN (Fig. 3I). Expression of adiponectin  
254 was overall higher in old injured RC at 5 days and 2 weeks post-TTDN compared to matched  
255 young injured RC (Fig. 3K) and significantly declined in old RC within 6 weeks after induction of

Commented [PB3]: These are young

Commented [PB4]: These are old

256 injury (Fig. 3K). These findings demonstrate that older mice develop more post-TTDN fatty  
257 degeneration of RC muscle tissue than young mice within 2 weeks. [There was no significant](#)  
258 [interaction between mouse age and injury in the expression levels of the tested adipogenic genes](#)  
259 [\(two-way ANOVA, p<0.01\).](#)

260

261

### 262 **PDGFR $\beta$ <sup>+</sup>PDGFR $\alpha$ <sup>+</sup> Fibro-adipogenic Progenitor Cells Have the Same Frequency in Non-** 263 **injured Young and Old RC Muscle Tissue**

264 The acceleration and increase in fibro-adipogenic response in old injured RC can be  
265 attributed to differences in the frequency of fibro-adipogenic progenitor cells between young and  
266 old RC. We have previously demonstrated that PDGFR $\beta$ <sup>+</sup>PDGFR $\alpha$ <sup>+</sup> progenitor cells contribute to  
267 tissue fibro-adipogenesis after injury<sup>12</sup> and therefore we used flow cytometry analysis to determine  
268 the frequency of PDGFR $\beta$ <sup>+</sup>PDGFR $\alpha$ <sup>+</sup> fibro-adipogenic precursors in RC of non-injured young  
269 (n=4, 3-4 months old) and old (n=3, 18-20 months old) mice. All PDGFR $\alpha$ <sup>+</sup> cells co-expressed  
270 PDGFR $\beta$  (Fig. 4A) and there was no significant difference in the frequency of fibro-adipogenic  
271 PDGFR $\beta$ <sup>+</sup>PDGFR $\alpha$ <sup>+</sup> cells between non-injured young and old RC tissue (Fig. 4B and 4C),  
272 implying that greater degeneration of injured old RC is attributable to the microenvironment,  
273 which would induce more active proliferation and differentiation of these fibro-adipogenic cells.  
274 Alternatively, or concomitantly, the intrinsic fibro-adipogenic potential of these  
275 PDGFR $\beta$ <sup>+</sup>PDGFR $\alpha$ <sup>+</sup> cells might increase with age (higher collagen production on a per-cell basis,  
276 for instance).

277 To test the former hypothesis, we performed multi-color immunofluorescence staining of  
278 PDGFR $\beta$  and PDGFR $\alpha$  in non-injured and injured young and old RC sections (Fig. 4D) and

279 quantified ~~the pixels color~~ representative of PDGFR $\beta$  expression, PDGFR $\alpha$  expression or  
280 PDGFR $\beta$  and PDGFR $\alpha$  co-expression. At each tested time point post-TTDN, a similar pixel  
281 fraction was measured for PDGFR $\beta$ , PDGFR $\alpha$  or co-expression of PDGFR $\beta$  and PDGFR $\alpha$ ,  
282 demonstrating that the fibrotic lesions are mainly populated by PDGFR $\beta^+$ PDGFR $\alpha^+$  cells (Fig.  
283 4E). The dynamic frequency of this subset was measured throughout the post-injury remodeling  
284 process of the RC and was shown to have a similar trend in both young and old RC at 5 days and  
285 6 weeks post-TTDN but not at 2 weeks post-TTDN (Fig. 4E). The frequency of  
286 PDGFR $\beta^+$ PDGFR $\alpha^+$  cells was increased within 5 days ( $p < 0.01$ ) as well as 2 and 6 weeks post-  
287 TTDN ( $p < 0.001$  and  $p < 0.00001$  respectively) in both young and old RC in comparison to non-  
288 injured muscle. However, a transient decrease in the frequency of PDGFR $\beta^+$ PDGFR $\alpha^+$  cells was  
289 measured only in young injured RC at 2 weeks post-TTDN (Fig. 4E). At 2 and 6 weeks post-  
290 TTDN, immuno-staining for PDGFR $\beta$  and PDGFR $\alpha$  illustrated larger fibrotic lesions in old RC  
291 tissue compared to young RC tissue post-injury (Fig. 4D), coinciding with greater measured color  
292 fraction of PDGFR $\beta^+$ PDGFR $\alpha^+$  cells in old degenerated RC at 2 and 6 weeks post-injury (Fig. 4E,  
293  $p < 0.01$  and  $p < 0.0001$  respectively) and thus implying a more robust pro-fibrotic environmental  
294 cues in old, injured RC muscle, which drives higher proliferation of fibro-adipogenic progenitor  
295 cells.

296

## 297 **DISCUSSION**

298 Rotator cuff tears are one of the most common musculoskeletal injuries and a substantial source  
299 of morbidity in elderly patients. Massive RC tears, in particular, are associated with muscle  
300 atrophy, fatty degeneration, and fibrosis. These degenerative processes interfere with tissue  
301 healing and are associated with poor surgical outcomes. In the present investigation, we found that

302 an increase in fibrosis and fat accumulation are associated with RC aging and substantially  
303 increased following tendon transection and denervation, in comparison to young RC. However,  
304 we measured a similar frequency of PDGFR $\beta$ <sup>+</sup>PDGFR $\alpha$ <sup>+</sup> pro-fibrotic cells in non-injured young  
305 and old RC, which indicates that the formation of larger fibrotic lesions in old injured RC can be  
306 attributed to microenvironmental cues, mediating increased expansion and/or differentiation of  
307 PDGFR $\beta$ <sup>+</sup>PDGFR $\alpha$ <sup>+</sup> fibrogenic cells. Alternatively, or in parallel, the intrinsic fibro-adipogenic  
308 potential of these PDGFR $\beta$ <sup>+</sup>PDGFR $\alpha$ <sup>+</sup> cells might increase with age. Supporting the notion that  
309 young fibro-adipogenic progenitors differ from their aged counterparts, it was recently reported  
310 that loss of secretion of WISP-1 from aged muscle-residing fibro-adipogenic progenitor cells  
311 impairs efficient muscle regeneration, but can be rescued by administration of young muscle-  
312 derived fibro-adipogenic progenitor cells.<sup>21</sup>

313 We found that older mice had greater amounts of fibrosis in RC muscle than younger mice,  
314 even prior to injury. In accordance, increase in collagen deposition has been observed in other  
315 muscle types of aged rats and mice. A two-fold increase in fibrotic lesions and collagen deposition  
316 was measured in hind limb soleus and extensor digitorum longus muscles of 2-year-old rats<sup>22</sup> as  
317 well as in the tibialis anterior muscles of 28-30-month-old mice<sup>23</sup> in comparison to matched young  
318 adult animals. Aging induced fibrosis was shown to relate to loss of muscle neuronal nitric oxide  
319 synthase that is associated with an increase in intramuscular leukocytes, especially M2a  
320 macrophages that can promote muscle fibrosis via arginase-mediated metabolism.<sup>24</sup> Aging of the  
321 bone marrow leads to a shift in myeloid cells in muscle toward the M2a phenotype that occurs  
322 independently of muscle age. This shift in macrophage phenotype can further promote muscle  
323 fibrosis during aging.<sup>24</sup>

324 Likewise, human muscles exhibit age-related increase in fat and connective tissue for arm  
325 and foot flexors as well as arm extensors,<sup>25</sup> reductions in the cross-sectional area of the quadriceps  
326 and hamstrings muscles of elderly men (65–77 years old), and concomitant increases in non-  
327 muscle tissue.<sup>26</sup>

328 We observed a transient progressive increase in collagen deposition within 2 weeks post  
329 injury followed by a decrease at 6 weeks post injury. These changes were more prominent in old  
330 injured RC and corresponded with increased numbers of fibrogenic PDGFR $\beta$ <sup>+</sup>PDGFR $\alpha$ <sup>+</sup> cells  
331 populating the fibrotic lesions of old injured RC. Several factors have been identified as  
332 modulators of collagen synthesis: while TGF $\beta$ 1, PDGF BB, endothelin 1, angiotensin II and IL-1  
333 stimulate collagen synthesis bFGF, NO, INF $\gamma$  and TGF $\alpha$  inhibit its production.<sup>27</sup> Possibly,  
334 differences in the levels of secreted factors between old and young injured RC are responsible for  
335 the more drastic changes in collagen production that are observed in old injured RC.

336 As opposed to the decline in collagen expression within 6 weeks post injury, the expression  
337 of adipogenic leptin was continuously increasing post injury with significantly higher expression  
338 in old RC at 6 weeks post TTDN. The leptin hormone is synthesized and secreted primarily by  
339 adipocytes and is present in serum in direct proportion to the amount of adipose tissue.<sup>28</sup>  
340 Accordingly, increased numbers of adipocytes were quantified over time following ~~induction of~~  
341 injury, ~~with~~ the highest count of adipocytes and, in correlation, highest ~~measured~~  
342 ~~being measured~~ in old injured RC at 6 weeks post injury.

343 We have recently demonstrated that co-expression of PDGFR $\beta$  and PDGFR $\alpha$  on a subset  
344 of muscle residing cells defines pro-fibrotic and scar residing fibrotic cells that directly contribute  
345 to the formation of fibrotic lesions in the chronically injured murine RC.<sup>29</sup> Our present findings  
346 demonstrate age-dependent differences in RC response to injury with enhanced contribution of

**Commented [PB5]:** This sentence is sort of difficult to understand in its original version



347 fibro-adipogenic PDGFR $\beta$ <sup>+</sup>PDGFR $\alpha$ <sup>+</sup> cells to muscle degeneration in aged mice. This can be  
348 explained in part by the results of studies assessing molecular and cellular changes within aged  
349 muscle that revealed several homeostatic perturbations, including decreased Notch signaling and  
350 increased activation of TGF $\beta$  signaling<sup>30</sup> that also mediates proliferation of myofibroblasts.<sup>31</sup>

351 Previous reports indicate that the type of experimental RC injury affects the rate of  
352 adipogenesis. Only when neurotomy was combined with tenotomy did rats develop severe fat  
353 accumulation similar to that seen in human patients.<sup>17</sup> Adipocyte infiltration in the supraspinatus  
354 muscle of the RC following tenotomy was observed in both adult and aged rats but was reported  
355 as not significantly different between young and old rats.<sup>32</sup> In another study, the infraspinatus was  
356 analyzed instead of the supraspinatus and tenectomy resulted in mild adipogenesis that appeared  
357 greater in aged rats compared to young rats.<sup>33</sup> Altogether, these findings suggest that the extent of  
358 adipogenesis differs between the supraspinatus and the infraspinatus and that the statistically  
359 significant contribution to increased adipogenesis that we have measured can be attributed to the  
360 infraspinatus. Still, a comprehensive statistical analysis should be performed to validate this  
361 assumption using a combined nerve and tendon RC chronic injury. However, there is also a  
362 difference between young and old rats in the expression of the stem cell regulatory proteins MyoD  
363 and Myf5, that facilitate the differentiation of stem cells into muscle cells.<sup>34</sup> Importantly, though,  
364 this study was performed in healthy aged rats as opposed to those with induced RC injury.

365 Altogether, these findings indicate that aged mice have a greater fibro-adipogenic response  
366 to massive RC tears. Future studies utilizing TTDN should use old mice to more accurately  
367 recapitulate the human condition. Clinically, cell-based therapies for muscular disease should  
368 consider not just the cells to be transplanted, but also the host milieu into which the cells will  
369 differentiate and grow.

370 **Limitations** Some limitations of this study are inherent in the model itself. Induction of an acute  
371 RC injury in a mouse may not be entirely representative of the chronic human clinical condition,  
372 and the shoulder joint being weight-bearing in rodents but not in humans must be taken into  
373 consideration. These differences may contribute to slightly different injury profiles and  
374 environmental milieux. In mice, neurotomy is essential for the induction of severe fat accumulation  
375 similar to that seen in human patients.<sup>17</sup> However, absence of functional nerve supply in this model  
376 would likely disrupt the evaluation of cell-based therapies aimed at regenerating functional human  
377 muscle. Additionally, to the best of our knowledge, there is no standard that currently exists for  
378 comparing cellular and genetic profiles in young and old mice and extrapolating these differences  
379 to humans. How degenerative changes in tissues seen between young and aged rodents translate  
380 to those seen over time in humans is not known. However, uncertainty about such cross-  
381 applicability exists for all research performed with animal models as proxies for clinical conditions  
382 in humans.

383

#### 384 **ACKNOWLEDGMENTS**

385 This work was supported by the Orthopaedic Research and Education Foundation.

386

387

388

389

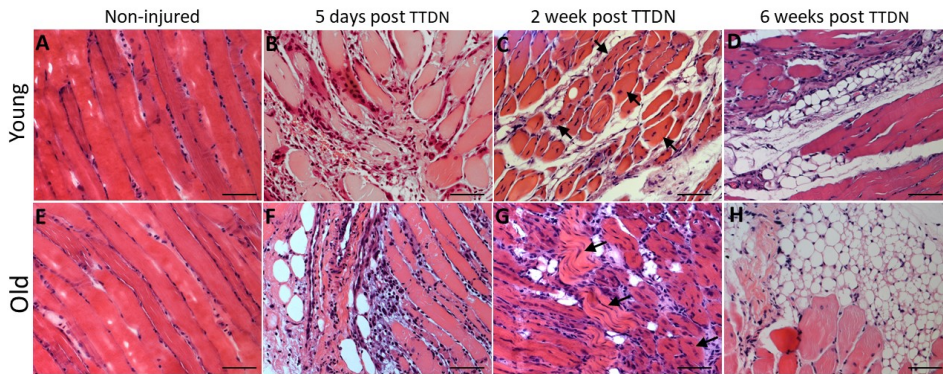
390

391

392

393

394



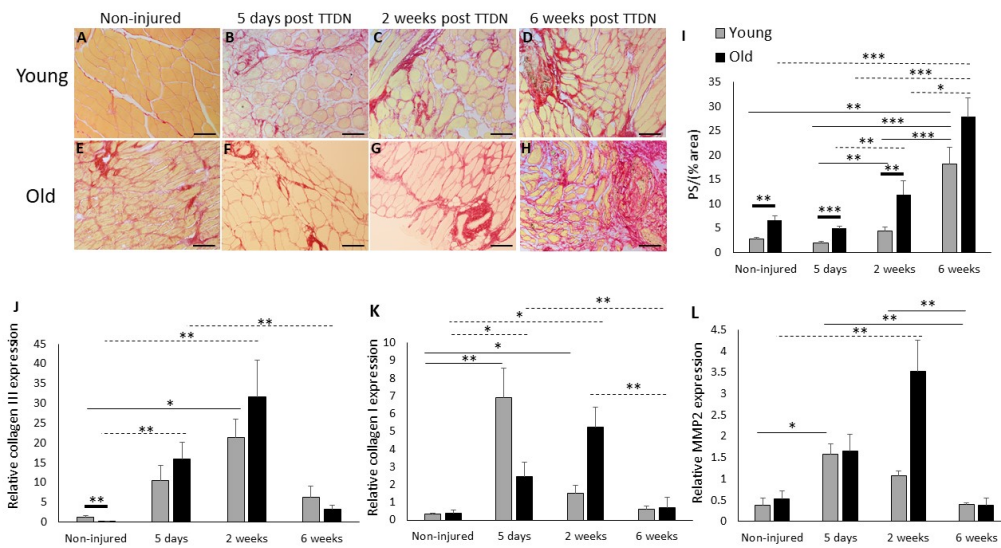
395

396 **Figure 1.** Representative hematoxylin-eosin stained sections demonstrating progressive fibro-  
397 adipogenic changes over time in mouse RC following tenotomy and denervation (TTDN). (A-D)  
398 Young (3-4 months) and (E-H) old (20-24 months) mouse muscle. (A and E) Normal muscle  
399 architecture of healthy, non-injured young (A) and old (E) mouse RC. (B and F) Increased  
400 cellularity and necrotic myofibers are seen at five days post-TTDN. (C and G) Myofiber  
401 regeneration is indicated by the centrally located nuclei within the myofibers (C and G; arrows) at  
402 2-weeks post-TTDN. (D and H) Increased fibro-adipogenic change is seen in the older cohort  
403 relative to the younger cohort at 6 weeks post-TTDN. Scale bar: 50 $\mu$ m.

404

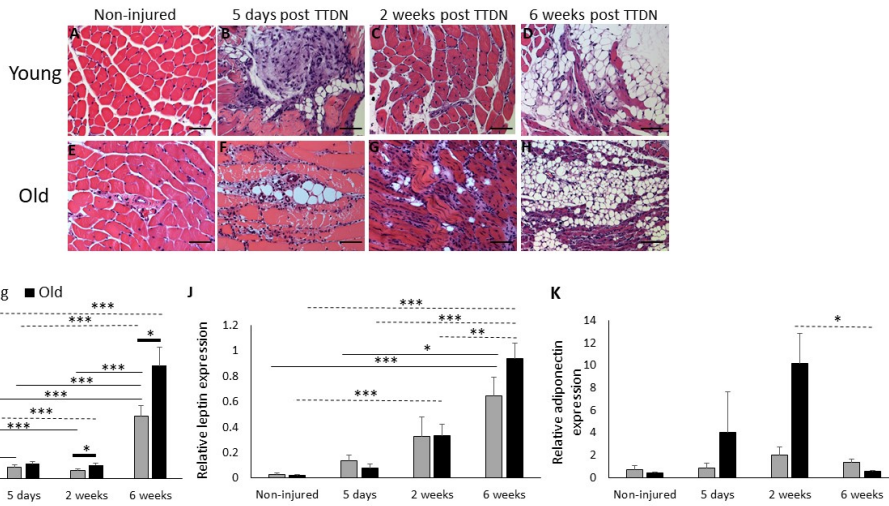
405

406



407  
 408 **Figure 2.** Picosirius red stain for histological visualization and quantification of collagen  
 409 deposition in RC tissue sections of young and old mice following TTDN. Collagenous tissue is  
 410 stained red and is visible between myofibers. (A-D) Young and (E-H) old muscle harvested from  
 411 non-injured mice (A and E) or at the indicated time points post-TTDN (B-G and F-H). (I) Pixel  
 412 fraction quantification of red collagen staining in young and old non-injured RC and at the  
 413 indicated time points post TTDN. (J-L) Relative expression of collagen III (J) collagen I (K) and  
 414 MMP-2 (L). expression. \* $p = 0.01$ ; \*\* $p = 0.005$ ; \*\*\* $p = 0.001$ .  $n =$  at least 3 mice per group. Solid  
 415 line represents comparisons between young RC tissue; Dashed line represents comparisons  
 416 between old RC tissue; Thick line represents comparisons between young and old RC tissues.  
 417 Scale bar: 50 $\mu$ m

418  
 419  
 420  
 421  
 422



424  
 425 **Figure 3.** Fat tissue accumulation in young and old RC post-TTDN. Hematoxylin-eosin stained  
 426 RC sections of (A-D) young and (E-H) old mice. Adipocyte accumulation in young (A-D) and old  
 427 (E-H) RC harvested from non-injured mice (A and E) or at the indicated time points post-TTDN  
 428 (B-G and F-H). (A and E) Normal muscle architecture of healthy, non-injured young (A) and old  
 429 (E) mouse RC. (I) Quantification of adipocytes in young and old non-injured RC and at the  
 430 indicated time points post TTDN. (J-K) Relative expression of leptin (J) and adiponectin (K). \**p*  
 431 = 0.01; \*\**p* = 0.005; \*\*\**p* = 0.001. n= at least 3 mice per group. Solid line represents comparisons  
 432 between young RC tissue; Dashed line represents comparisons between old RC tissue; Thick line  
 433 represents comparisons between young and old RC tissues. Scale bar: 50µm.

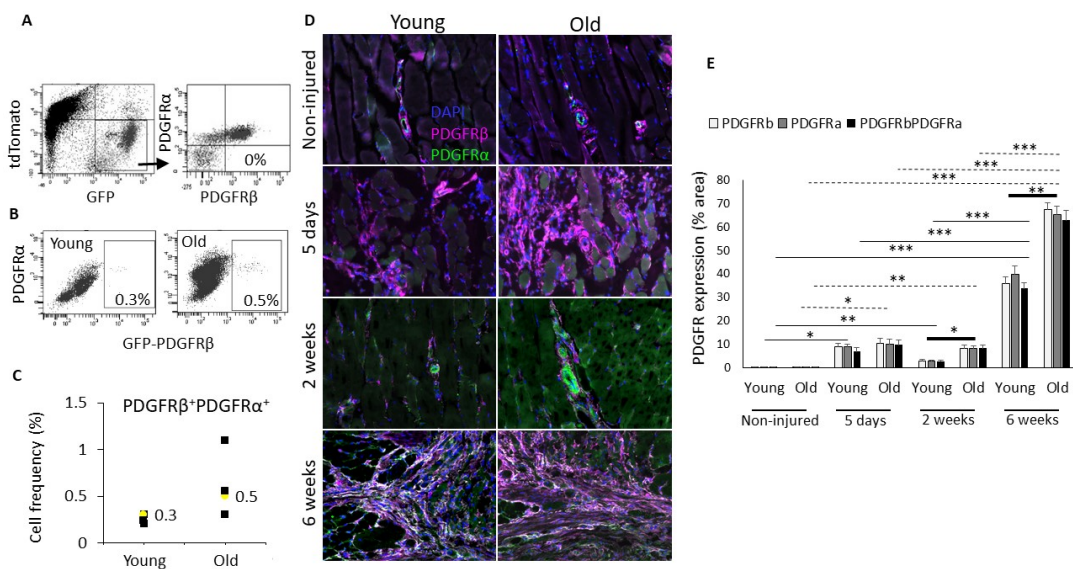
434

435

436

437

438



439 **Figure 4.** Quantification of PDGFR expression in chronically degenerating RC. (A)  
 440 Representative flow cytometry dot plots of PDGFR $\beta^+$ /PDGFR $\alpha^+$  cell subsets. (B-C) Frequency  
 441 of PDGFR $\beta^+$ PDGFR $\alpha^+$  cells in non-injured young and old RC. (D) Representative images of  
 442 PDGFR $\beta$  (pink) and PDGFR $\alpha$  (green) immuno-staining of non-injured RC and at the indicated  
 443 time points post-TTDN. Co-localization of PDGFR $\beta$  and PDGFR $\alpha$  is seen in light green and white.  
 444 (E) Quantification of pink (PDGFR $\beta$  expression), green (PDGFR $\alpha$  expression) and light  
 445 green/white (PDGFR $\beta$  and PDGFR $\alpha$  co-expression) pixel fraction per imaged area of stained RC  
 446 sections. No significant difference was observed between PDGFR $\beta$  and PDGFR $\alpha$  pixel fraction.  
 447 \* $p = 0.01$ ; \*\* $p = 0.001$ ; \*\*\* $p = 0.00001$ ;  $n = 3$  mice per group. Solid line represents comparisons  
 448 between young PDGFR $\beta^+$ PDGFR $\alpha^+$ , dashed line represents comparisons between old  
 449 PDGFR $\beta^+$ PDGFR $\alpha^+$ , thick line represents comparisons between old and young  
 450 PDGFR $\beta^+$ PDGFR $\alpha^+$ .

451 **REFERENCES**

- 452 1. Smith, M.A. & Smith, W.T. Rotator cuff tears: an overview. *Orthop Nurs* **29**, 319-322;  
453 quiz 323-314 (2010).
- 454 2. Aurora, A., McCarron, J., Iannotti, J.P. & Derwin, K. Commercially available extracellular  
455 matrix materials for rotator cuff repairs: state of the art and future trends. *J Shoulder Elbow*  
456 *Surg* **16**, S171-178 (2007).
- 457 3. Galatz, L.M., Griggs, S., Cameron, B.D. & Iannotti, J.P. Prospective longitudinal analysis  
458 of postoperative shoulder function : a ten-year follow-up study of full-thickness rotator cuff  
459 tears. *J Bone Joint Surg Am* **83-A**, 1052-1056 (2001).
- 460 4. Goldberg, B.A., Nowinski, R.J. & Matsen, F.A., 3rd Outcome of nonoperative  
461 management of full-thickness rotator cuff tears. *Clin Orthop Relat Res*, 99-107 (2001).
- 462 5. Le, B.T., Wu, X.L., Lam, P.H. & Murrell, G.A. Factors predicting rotator cuff retears: an  
463 analysis of 1000 consecutive rotator cuff repairs. *Am J Sports Med* **42**, 1134-1142 (2014).
- 464 6. Park, J.G. *et al.* Rotator Cuff Repair in Patients over 75 Years of Age: Clinical Outcome  
465 and Repair Integrity. *Clin Orthop Surg* **8**, 420-427 (2016).
- 466 7. Picavet, H.S. & Schouten, J.S. Musculoskeletal pain in the Netherlands: prevalences,  
467 consequences and risk groups, the DMC(3)-study. *Pain* **102**, 167-178 (2003).
- 468 8. Boileau, P. *et al.* Arthroscopic repair of full-thickness tears of the supraspinatus: does the  
469 tendon really heal? *J Bone Joint Surg Am* **87**, 1229-1240 (2005).
- 470 9. Charousset, C., Bellaiche, L., Kalra, K. & Petrover, D. Arthroscopic repair of full-thickness  
471 rotator cuff tears: is there tendon healing in patients aged 65 years or older? *Arthroscopy*  
472 **26**, 302-309 (2010).
- 473 10. Downie, B.K. & Miller, B.S. Treatment of rotator cuff tears in older individuals: a  
474 systematic review. *J Shoulder Elbow Surg* **21**, 1255-1261 (2012).
- 475 11. Gumina, S. *et al.* The impact of aging on rotator cuff tear size. *Musculoskelet Surg* **97**  
476 **Suppl 1**, 69-72 (2013).
- 477 12. Feng, S., Guo, S., Nobuhara, K., Hashimoto, J. & Mimori, K. Prognostic indicators for  
478 outcome following rotator cuff tear repair. *J Orthop Surg (Hong Kong)* **11**, 110-116 (2003).
- 479 13. Fehring, E.V., Sun, J., VanOeveren, L.S., Keller, B.K. & Matsen, F.A., 3rd Full-  
480 thickness rotator cuff tear prevalence and correlation with function and co-morbidities in  
481 patients sixty-five years and older. *J Shoulder Elbow Surg* **17**, 881-885 (2008).
- 482 14. Hermans, J. *et al.* Does this patient with shoulder pain have rotator cuff disease?: The  
483 Rational Clinical Examination systematic review. *JAMA* **310**, 837-847 (2013).
- 484 15. Uysal, A.C. & Mizuno, H. Differentiation of adipose-derived stem cells for tendon repair.  
485 *Methods Mol Biol* **702**, 443-451 (2011).
- 486 16. Kawiak, J. *et al.* Contribution of stem cells to skeletal muscle regeneration. *Folia*  
487 *Histochem Cytobiol* **44**, 75-79 (2006).
- 488 17. Kim, H.M., Galatz, L.M., Lim, C., Havlioglu, N. & Thomopoulos, S. The effect of tear  
489 size and nerve injury on rotator cuff muscle fatty degeneration in a rodent animal model. *J*  
490 *Shoulder Elbow Surg* **21**, 847-858 (2012).

- 491 18. Liu, X. *et al.* A mouse model of massive rotator cuff tears. *J Bone Joint Surg Am* **94**, e41  
492 (2012).
- 493 19. Dutta, S. & Sengupta, P. Men and mice: Relating their ages. *Life Sci* **152**, 244-248 (2016).
- 494 20. Jackson, S.J. *et al.* Does age matter? The impact of rodent age on study outcomes. *Lab*  
495 *Anim* **51**, 160-169 (2017).
- 496 21. Lukjanenko, L. *et al.* Aging Disrupts Muscle Stem Cell Function by Impairing  
497 Matricellular WISP1 Secretion from Fibro-Adipogenic Progenitors. *Cell Stem Cell* **24**,  
498 433-446 e437 (2019).
- 499 22. Alnaqeeb, M.A., Al Zaid, N.S. & Goldspink, G. Connective tissue changes and physical  
500 properties of developing and ageing skeletal muscle. *J Anat* **139 ( Pt 4)**, 677-689 (1984).
- 501 23. Wood, L.K. *et al.* Intrinsic stiffness of extracellular matrix increases with age in skeletal  
502 muscles of mice. *J Appl Physiol (1985)* **117**, 363-369 (2014).
- 503 24. Wang, Y., Wehling-Henricks, M., Samengo, G. & Tidball, J.G. Increases of M2a  
504 macrophages and fibrosis in aging muscle are influenced by bone marrow aging and  
505 negatively regulated by muscle-derived nitric oxide. *Aging Cell* **14**, 678-688 (2015).
- 506 25. Rice, C.L., Cunningham, D.A., Paterson, D.H. & Lefcoe, M.S. Arm and leg composition  
507 determined by computed tomography in young and elderly men. *Clin Physiol* **9**, 207-220  
508 (1989).
- 509 26. Overend, T.J., Cunningham, D.A., Kramer, J.F., Lefcoe, M.S. & Paterson, D.H. Knee  
510 extensor and knee flexor strength: cross-sectional area ratios in young and elderly men. *J*  
511 *Gerontol* **47**, M204-210 (1992).
- 512 27. Rekhter, M.D. Collagen synthesis in atherosclerosis: too much and not enough. *Cardiovasc*  
513 *Res* **41**, 376-384 (1999).
- 514 28. Considine, R.V. Human leptin: an adipocyte hormone with weight-regulatory and  
515 endocrine functions. *Semin Vasc Med* **5**, 15-24 (2005).
- 516 29. Jensen, A.R. *et al.* Neer Award 2018: Platelet-derived growth factor receptor alpha co-  
517 expression typifies a subset of platelet-derived growth factor receptor beta-positive  
518 progenitor cells that contribute to fatty degeneration and fibrosis of the murine rotator cuff.  
519 *J Shoulder Elbow Surg* **27**, 1149-1161 (2018).
- 520 30. Cholok, D. *et al.* Traumatic muscle fibrosis: From pathway to prevention. *J Trauma Acute*  
521 *Care Surg* **82**, 174-184 (2017).
- 522 31. Kim, J. & Lee, J. Role of transforming growth factor-beta in muscle damage and  
523 regeneration: focused on eccentric muscle contraction. *J Exerc Rehabil* **13**, 621-626  
524 (2017).
- 525 32. Farshad, M., Wurgler-Hauri, C.C., Kohler, T., Gerber, C. & Rothenfluh, D.A. Effect of age  
526 on fatty infiltration of supraspinatus muscle after experimental tendon release in rats. *BMC*  
527 *Res Notes* **4**, 530 (2011).
- 528 33. Gumucio, J.P. *et al.* Aging-associated exacerbation in fatty degeneration and infiltration  
529 after rotator cuff tear. *J Shoulder Elbow Surg* **23**, 99-108 (2014).



530 34. Plate, J.F. *et al.* Age-related changes affect rat rotator cuff muscle function. *J Shoulder*  
531 *Elbow Surg* **23**, 91-98 (2014).  
532